MODULATING COATABILITY OF SUPERFICIALLY METAL MESH INCORPORATED POLYMER COMPOSITES VIA OPTIMIZED GRIT BLASTING AND MACHINE VISION INSPECTION

Sedigh Rahimabadi*, P., Shokri, S., Kwok, T.H. and Hojjati, M.
Department of Mechanical, Industrial, and Aerospace Engineering, Concordia University
Montreal, Quebec, Canada
* Corresponding author (pooria.sedigh@gmail.com)

Keywords*: Composite Processing, Grit Blasting, Vision Inspection*

ABSTRACT

Despite many advantages of fiber reinforced polymer composites, which make them suitable for various industries such as aerospace and energy sector, they possess some limitations. Low thermal and electrical conductivity and low erosion resistance are some of the issues that can be resolved through surface coating, and especially metallization. For this purpose, incorporation of metal wire mesh in the composites forms a superficial anchor for deposition of metals using thermal sprays, which has been proven to be an effective method. However, obtaining a proper surface coating is yet dependent on the exposure level of fully resin-covered metal mesh by grit blasting before the coating process. In this paper, optimization of grit blasting parameters and introduction of operational parameter maps for preventing damage to the composite during grit-blasting are carried out. An in-house automated sample holder for grit blasting process is designed and manufactured for accurate control of grit blasting process. Then, a systematic experimentation is designed to primarily investigate the effect of grit blasting pressure, time and stand-off distance at three levels on the exposure level of metal mesh. Portable digital microscopy and conventional optical microscopy are employed to inspect the composite surface and to measure the level of material removal at each processing conditions. A machine vision algorithm is developed for the digital microscopy, not only to speed-up and to enhance the accuracy of inspection, but also to introduce an economical, non-destructive tool for in-situ characterization. According to the results, it is practical to achieve a desirable metal mesh exposure following the optimized grit-blasting parameters. Moreover, the computer-aided inspection can enormously contribute to realization of uniform, and efficient grit blasting in industrial application for huge structural parts such as wind turbine blades and airplane wings.

1 INTRODUCTION

Fiber reinforced polymer composites (FRPCs) have prevailed over other engineering materials in several industry applications, such as aerospace, automobile, chemical containers, biomedical, leisure equipment, electronics, maritime [1], civil infrastructures [2], and even energy sector [3, 4]. This wide range of applications has been realized as a result of significant specific strength and stiffness, brilliant fatigue resistance, good corrosion resistance, and flexibility in manufacturing methods based on properties and geometrical features in demand [5]. However, in-service performance of FRPC components has been affected by disorder leading to failure and fatal accidents. Icing and strike of lightening on airplane wings made of FRPCs due to low thermal and electrical conductivity [6, 7], both high-velocity impact causing damage on radome of planes and low-velocity impact fatigue [8], flammability of structures such as ship hulls [9], and erosion damage of wind turbine blades [10], are among the drawbacks of FRPCs. Therefore, further development of this class of material is required to address these issues and insure their safe

applications. Considering that these phenomena arise from the surface of components, surface coating and especially surface metallization is a promising resolution.

Surface coating techniques such as thermal spray (TS), vapor deposition, electroless deposition and sol-gel has been employed to deposit surface protection coatings for FRPCs [11]. Amid these methods, TS methods have attracted more attention because of their capabilities to form thick and thin functional films with higher deposition rate and in an economical manner. Nevertheless, the successful application of TS is still in debate. Fundamentally, TS processes involve propulsion of molten and/or semi-molten particles impinging the target substrate with a high speed[12], both of which can be destructive for the thermosetting polymeric matrix of substrate sensitive to high temperature and erosion [13, 14]. Therefore, aside from spraying a mixture of thermoplastic polymer/metal powders [15], suitable surface preparation prior to the coating process is required to assure deposition of protective film with good adhesion and avoid degradation of FRPC substrate. In this regard, electroless plating of a bond coat [16], application of garnet sand/adhesive film [17], manual spraying of metallic powders [13], and embedding a metal wire mesh on the surface of FRPC [18] have been successfully implemented. The main distinguishing characteristics of these methods is the number of excessive processes involved prior to the coating, and the obtained adhesion strength of the deposited film. Conforming to the results, integrating a metal wire mesh is not only superior in terms of anchoring the TSed coating, but also it does not coerce an extra step into the coating process. Indeed, the integration of the metal mesh into the FRPC is carried out during fabrication of the component by laying up the mesh on outermost surface. In this manner, the thermosetting resin can flow through the mesh covering it completely during the curing step. Thereafter, the fabricated substrate is prepared for TS process by grit-blasting (i.e., spray of abrasive particles using compressed air on the surface of a part) to clean it from contamination and increasing roughness (and exposing the metal mesh in this case) for better mechanical anchorage of the coating similar to other substrates [19].

Accordingly, the effect of mesh size on the adhesion strength of the deposited coatings was investigated indicating metal wire mesh 200 providing higher adhesion strength than metal mesh 400 [18]. However, the influence of grit-blasting process on the exposure level of metal mesh has not been investigated. This parameter is crucially important to ascertain availability of metallic anchor for deposition TS particles and formation of coating with robust adhesion. The grit-blasting process involves several variables such as grits size, shape, and material, blasting pressure, stand-off distance and angle, as well as number of passes (or time). Also, the process is carried out manually and it is therefore dependent on the operator's skill. In this study, an automated setup is employed to systematically investigate the effect of grit-blasting factors on the exposure level of metal wire in superficially integrated metal wire mesh/FRPC. The extracted results from digital microscopy are implemented to generate mathematical models and safe operational windows. Moreover, the results are utilized to develop a computer vision inspection method for in-situ, non-destructive characterization via digital microscopy in industrial applications. The remainder of this paper is organized as follows; Section 2 explains the theoretical aspect, experimentation, and analysis path. Section 3 is put forward to present the results and discuss the effect of variables on the system response. Ultimately, the conclusion and outlook of this study is summarized in section 4.

2 Methodology and Experimentation

2.1 Fabrication of Metal Wire Mesh/FRPC

Square plates of carbon fiber reinforced polymers (CRFPs) with dimensions of 29 cm × 31.5 cm were fabricated from CYCOM® 977-2 prepregs with stacking sequence of $[0]_{20}$ accompanied by a stainless steel 316 metal wire mesh laid up on the top and fixed with aluminum caul plate. The vacuum bagged system is then cured in autoclave at 180 °C

for 6 hours under the pressure of 70 psi, while the vacuum maintained. Subsequently, the resin with reduced viscosity flowed upward through the mesh and integrating it in the composites structure, as observable in Figure 1. Aiming to extract the exposure level of metal wires after grit-blasting via digital microscopy of the top instead of cross-section, it is vital to establish a relation between top and cross-section view. Interpolating a polynomial describing height of polymer after grit-blasting as a function of wire exposure length, it is possible to correlate the mesh exposure level inspecting the samples from top-view, as observable in Figure 2. In this regard, coordination's of several points were extracted from cross-sectional view by "ImageJ" software and polynomial interpolated as:

$$h = 108.77(\frac{x}{2})^4 - 58.608\left(\frac{x}{2}\right)^3 + 8.495(\frac{x}{2})^2 - 0.067(\frac{x}{2}) + 0.06 \quad (1)$$

where *x* (µm) is the average wire exposure length, and *h* (µm) denotes the height of polymer removed or exposure level. It is worthwhile of mention that ideally, where the metal wire mesh displays exact dimensions with no disorder, the maximum value of *x* would be *Lc*, providing less than 50% exposure.

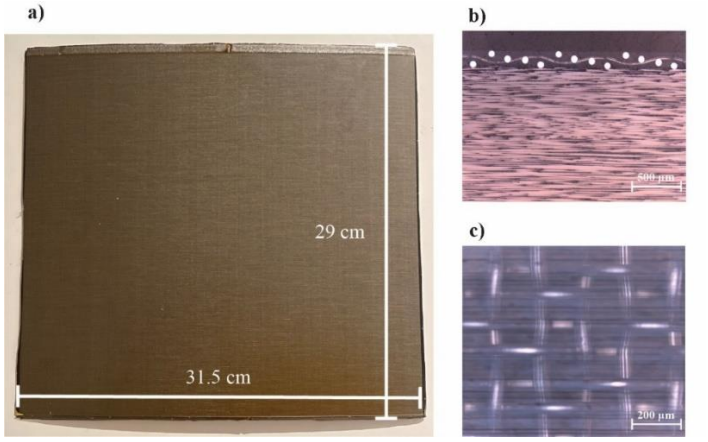

Figure 1. a) As-fabricated metal mesh/CFRP plate, b) and C) cross-sectional and top optical microscopy of mesh covered by resin and integrated in the structure of the composite.

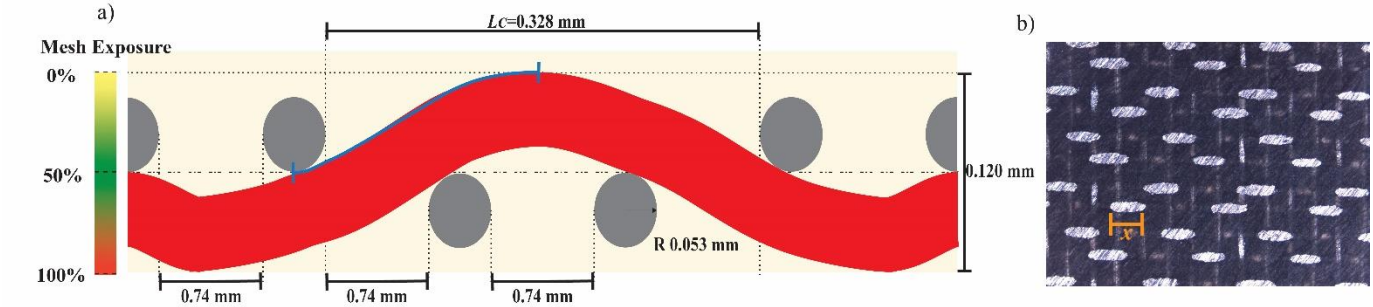

Figure 2. a) Schematic representation of metal mesh/epoxy denoting the dimensions and color bar illustrating mesh exposure. b) Microscopy of sand-paper polished sample demonstrating exposed wires. The blue curve in a) is subjected for interpolation.

2.2 Design and Assembly of Automated Grit-blasting Setup

To control the angle and stand-off distance of grit-blasting gun from sample, and perform a uniform grit-blasting, the homemade, automated setup observable in Figure 3(a) is designed and assembled. Two motorized linear

actuator stages transverse to each other provide passage of sample in both horizontal and vertical direction with travel range of 20 cm. An adjustable pipe clamp as gun holder is installed on rails perpendicular to the sample stage allowing control of the angle and stand-off distance. The motors are programmed employing a developed "Arduino" code enabling travel of sample stage across the gun, with the pattern in Figure 3(b), at the speed range of 3 to 7 mm/s and adjustable number of passes. Further, several vinyl protective films were applied on the actuator stages and motors to protect them from abrasive environment of grit-blasting cabinet.

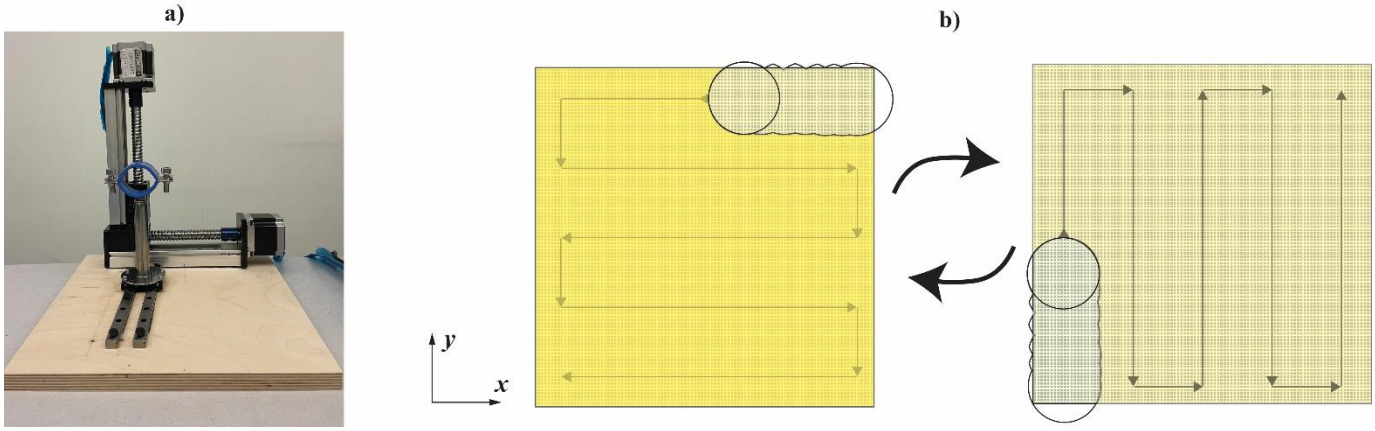

Figure 3. a) The automated grit-blasting setup, b) the movement pattern of sample stage across from grit-blasting gun.

2.3 Grit-blasting Process

proceeding with the grit-blasting process, the setup is installed in "ECO-420 sandblasting cabinet for light-duty application". Pursuant to previous studies [18], Al_2O_3 grits with a mesh size of 80 (particle size of 180 µm) was utilized for grit-blasting with the pressure (*P*) of 76 psi and distance (*d*) of 6 cm for 150 sec as the initial experiment. However, due to variability of the results, it is attempted to investigate the effect of *P*, *d*, and time (*t*) on the exposure level of wires, in a wide range of values. In this regard, each parameter is studied at three different levels of *P* = 60, 80, 100 psi, *d* = 7, 10, 13 cm, and *t* = 60, 120, 180 sec. These values are determined based on trial and errors and considering the safety issues. Moreover, grit-blasting angle is kept constant at 90°, and Al_2O_3 grits with a mesh size of 80 are employed, as increasing the particle size could adversely affect the accuracy and reducing particle size could rise safety concerns by scattering of dust and grits out of the cabinet.

2.4 Microscopy Characterization

For the purpose of characterization from top-view, "Skybasic handheld digital microscope" is utilized providing high resolution images with a magnification of 50×-1000×. The microscopy process is conducted employing adjustable stand holder allowing for obtaining images with the same magnification and quality. Acquiring images from five random spot on each grit-blasted samples enabled extracting the length of several exposed wires via "ImageJ", which in turn provide the average exposure length. Moreover, the samples were cut in half, in order to investigate the validation of proposed model based on top-view, by optical microscopy of cross-section and measuring mesh exposure level.

2.5 Computer Vision Inspection

As a first step for developing a system for automated inspection of grit-blasted metal mesh/FRPCs, developing image processing and feature extraction techniques is invaluable. Herein, the digital microscopy images of grit-blasted samples are subjected to an adaptive binarization process for segmentation and distinguishing exposed metal wires

from residues of polymer, considering different light reflection of them. With this aim, the colored images are converted to single channel gray-scale ones, followed by application of a bilateral filter for reduction of noise and maintaining the coherency of the images simultaneously. Thereafter, a black-and-white binarization were employed by "Otsu's adaptive thresholding" method to increase the accuracy for the segmentation. Also, a closing operator is implemented for further eliminating the high-frequency noise by dilating and eroding image segmentations. Afterwards, neighboring pixels with the same attribute (color) are clustered, which exhibit the residual polymers and exposed metal wires, separately. Thus, plotting cluster size distribution allows a classification for differentiating under-blasted, proper-blasted, and over-blasted regions.

3 Results and Discussions

3.1 Characterization and Parametric Analysis

The optimization and generation of operational windows are carried out through developing a regression model based on the data extracted from digital microscopy of grit-blasted samples. Figure 4 depicts the microscopy and distribution of wire exposure lengths of under-blasted (mesh exposure level below 35%), proper-blasted (mesh exposure level in the range of 35-60%), and over-blasted (mesh exposure level beyond 60%) samples, which provides the corresponding *x value*. Accordingly, not all the histograms show a normal distribution of exposed wire length, which is due to inaccuracies related to blasting process. To illustrate, clogging of grits in the gun leads to lack of grit-blasting of a spot, while getting unclogged at the next zone causes higher abrasion. Moreover, the existence of impurities and size distribution of grits affect the inconsistent state of blasting from one spot to another. it is therefore assumed that the behavior of wire length exposure is normal for simplification purpose. Employing equation 1, the exposure level of metal mesh is calculated. Also, the calculated exposure level is further validated using optical microscopy of the cross-section of grit-blasted samples (Figure 5.a-c).

As, it is observable in Figure 4, it is not practical to extract *x* values for over-blasted samples due to either deteriorations in metal mesh pattern or complete erosion of it. Therefore, the mesh exposure level is estimated based on the deterioration of metal mesh and composite, and with respect to the calculated mesh-exposure level of under-blasted and proper-blasted samples. The best regression model is fitted employing a box-cox transformation, which eventually provides both accuracy for predicted mesh exposure at all levels, and reasonable confidence intervals. The corresponding coefficients for the transformed response regression model are highlighted in Table 2. With respect to number of variables, comprehension of the results is complicated in 3D maps. Therefore, 2D surface window maps are developed to demonstrate the mesh exposure level as a function of *P* and *t* at various distances (Figure 6) since the two latter parameters are more vital in terms of optimization of the process for industrial application. As observable, increasing *d* from 7 to 11 cm highly widen the safe window (30-60% mesh exposure) for grit-blasting with moderate *P* and *t* (i.e., 70-80 psi for a duration of 90-150 sec). Whereas, further increasing d requires higher *P* and *t* for achieving appropriate mesh exposure. Therefore, it can be expected that parameter sets of *P*=75-85 psi, *d*= 10-11 cm, and *t*=90-120 sec, not only provide a proper mesh exposure level (35-55%), but also avoid destruction of mesh and composite with a good degree of safety. This is crucial, because an under-blasted part can be further grit-blasted to achieve the proper mesh exposure state, on the contrary to over-blasted part.

3.2 Morphological Analysis

In addition to the mesh exposure level, shape and roughness of the exposed wires is an important parameter as they undergo deformation and erosion during grit-blasting. Analyzing the shape of wires employing optical microscopy (Figure 5.d-f), it can be deduced that the erosion of metal wires by Al_2O_3 grits is an inevitable issue,

nevertheless the degree of deformation/erosion can be controlled through modulating *P*. In this regard, grit-blasting with a *P* of 60 psi leads to erosion of wires while they almost maintain their initial round shape. Increasing *P* to 80, the wires undergo a mixture of deformation and erosion promoting available metallic substrate with a high roughness for deposition of TSed particles. However, further increasing *P* causes higher erosion and even local destruction of mesh. Thus, maintaining a moderate *P* is necessary to obtain a highly coatable metal mesh/FRPC.

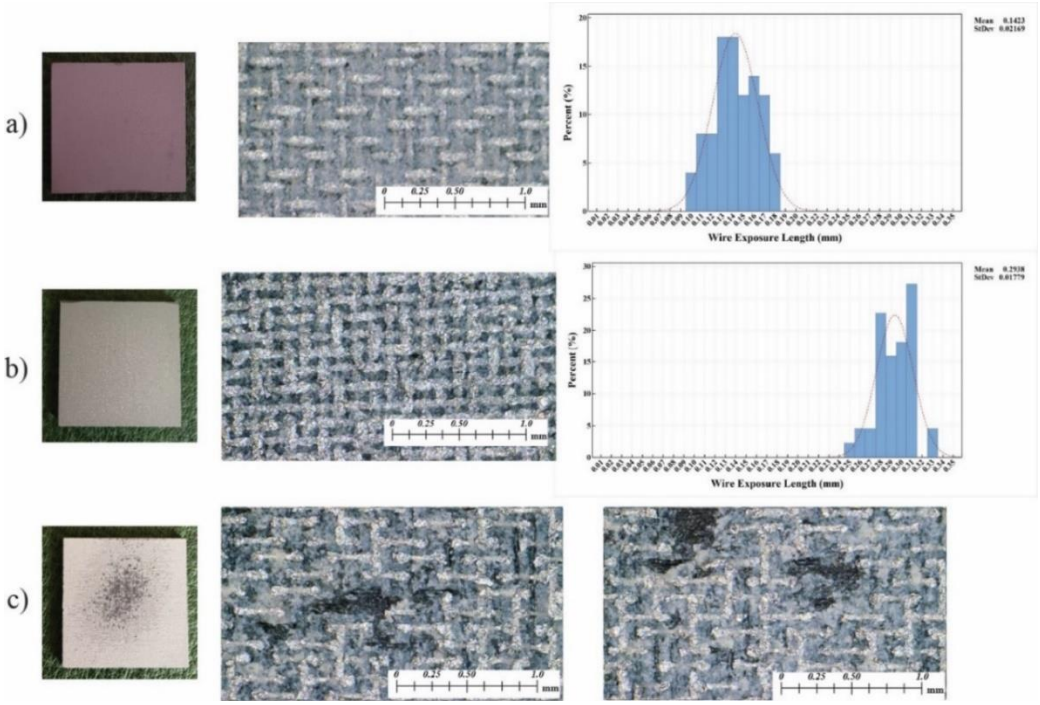

Figure 4. a) and b) images of under-blasted and proper-blasted samples along with the top-view digital microscopy and distribution of exposed wires length. c) Image of over-blasted sample and its top-view digital microscopy showing destruction of mesh pattern.

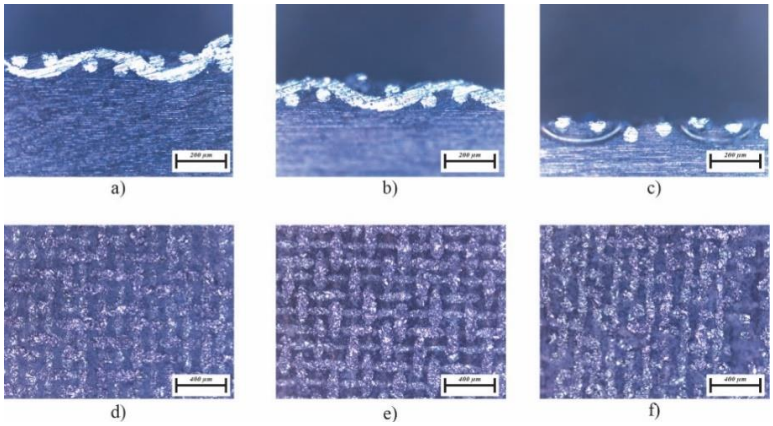

Figure 5. Optical microscopy of a) under-blasted, b) proper-blasted, and c) over-blasted validating the mesh exposure level and destruction of mesh. Top view microscopy of the samples demonstrating the effect of *P* on the erosion/deformation of wires.

Table 1. coefficients for transformed response regression model with λ=0.

Term	Coefficient	P-Value
P (psi)	0.05584	0.000
d (cm)	-0.0642	0.203
t (sec)	0.01628	0.002
P (psi)*d (cm)	-0.001216	0.095
P (psi)*t (sec)	-0.000141	0.007
d (cm)*t (sec)	0.000226	0.501

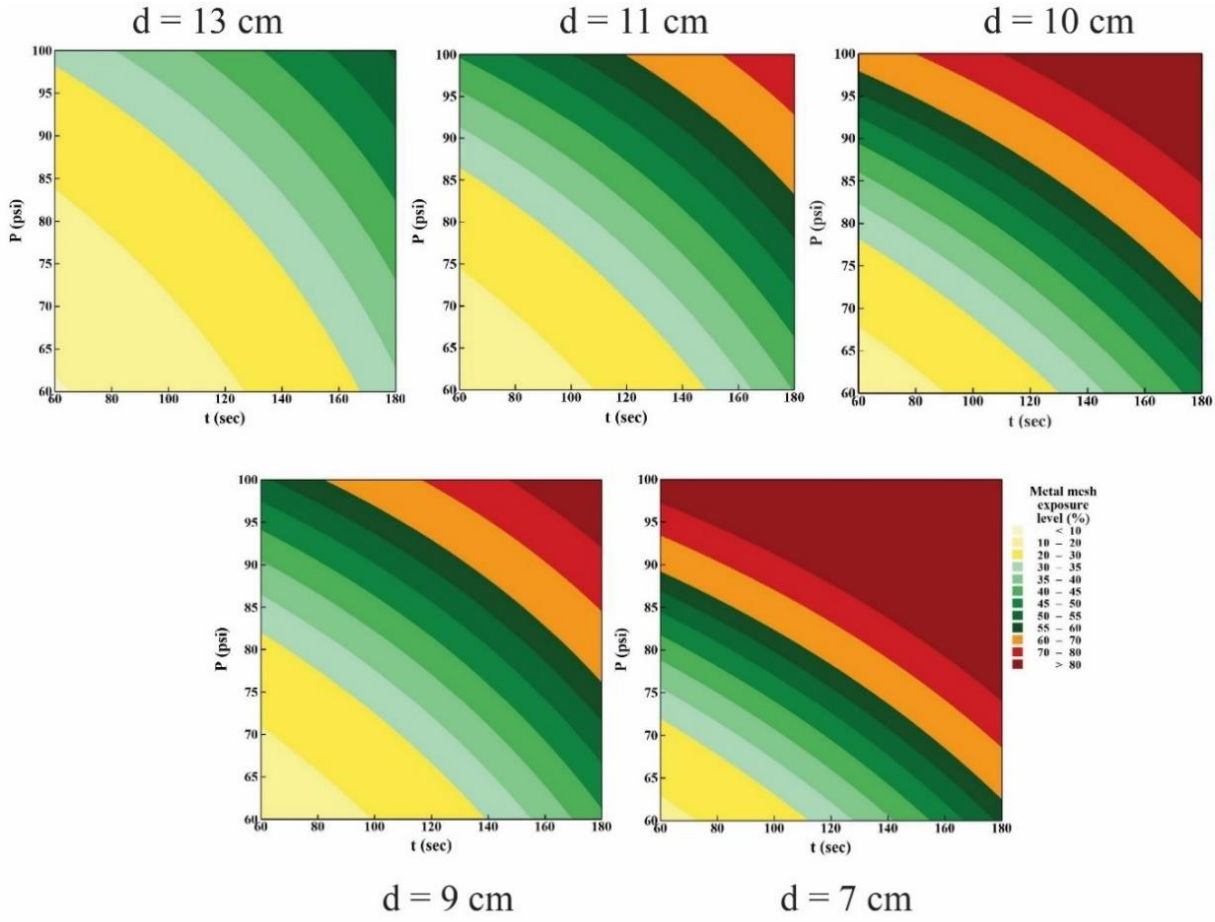

Figure 6. Developed operational grit-blasting window for prediction and optimization of mesh exposure level as a function of *P* and *t*, at various distances.

3.3 Computer-aided Analysis

Categorizing the grit-blast state into three sub-group is realized by employing a rather simplified image processing method. Figure 7 depicts the input, black-and- white binarized, and resin clustered images of under-blasted, proper-blasted, and over-blasted samples. With respect to the shape of the metal wire mesh, ideally, it can be expected that a grit-blasted sample demonstrate small, squared shape resin clusters in between the metal wires, in contrast to the under-blasted and over-blasted samples with resin clusters comprising larger areas and marginal wires. As it can be observed, the results of the resin clustering carried out in this study are in good agreement with the

expectations. For the proper-blasted samples, although the resin clusters do not exhibit a fully square shape, they pose smaller size and are distributed between the exposed metal wires. Moreover, the under-blasted and over-blasted samples exhibit very large resin clusters denoting either lack of wire exposure or destruction of wires. The distinguishing characteristic between under-blasted and over-blasted can be defined with respect to the width of mesh clusters, which are smaller in the case of under-blasted state.

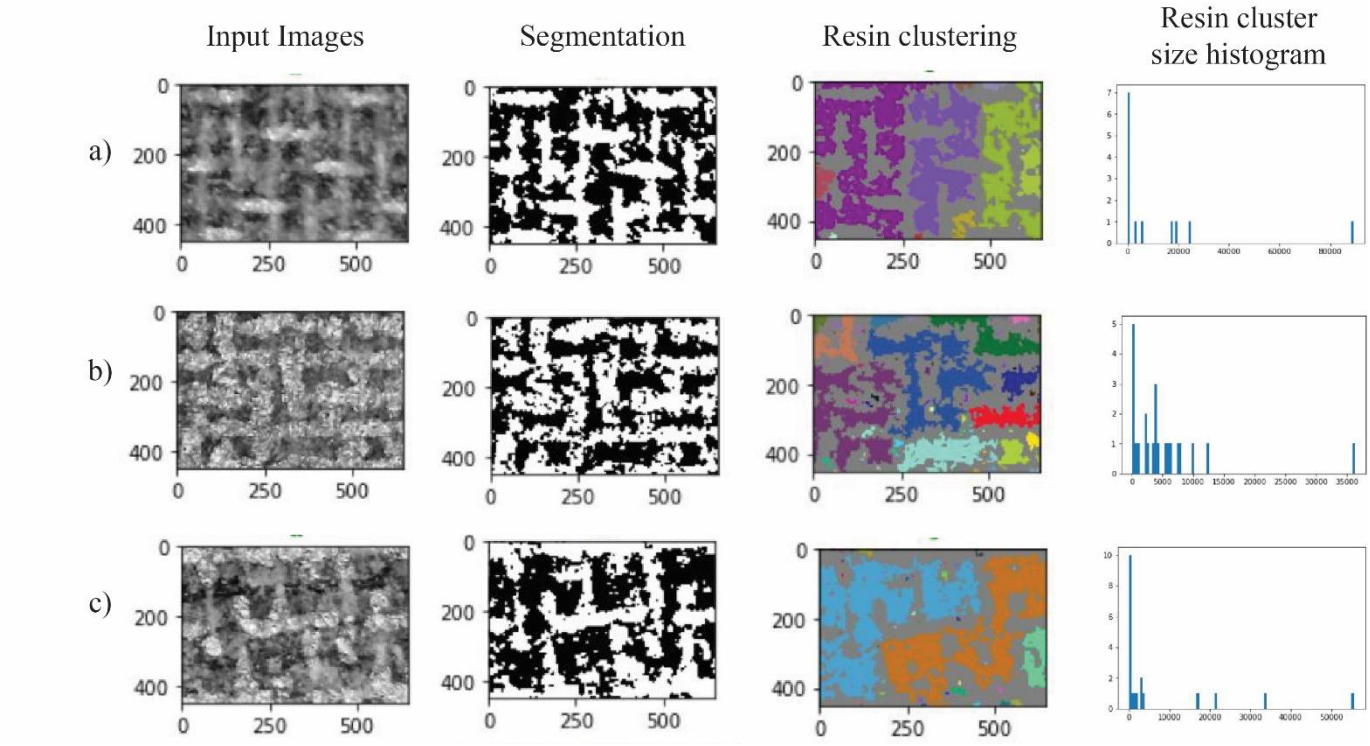

Figure 7. Top-view digital microscopy, black-and-white binarized, and resin clustering images of a) under-blasted, b) proper-blasted, and c) over-blasted samples.

4 Conclusion and Outlook

In summary, preparing the surface of metal mesh/FRPC for TS coating through grit-blasting process is parametrically investigated in this study to generate operational windows and develop a non-destructive analysis technique utilizing portable digital microscopy and image processing. It is revealed the grit-blasting the system with Al_2O_3 angular grits with a mesh size of 80 can be optimally carried out implementing a parameter set in the range of P=75-85 psi, d= 10-11 cm, and t=90-120 sec. This way, it is not only possible to form a highly coatable exposed metal mesh integrated in the composite, but also to avoid erosion of metal mesh and failure of the component. Moreover, it is established that a portable digital microscopy can be utilized for inspection of grit-blasted component either manually or computationally. Exploring other grits materials and sizes are highly encouraged for further advancement of the process. The computer-aided analysis utilized in this study is being further developed to realize automation of grit-blasting process based on the mesh exposure level computation and determining second step grit-blasting parameters for under-blasted zones.

5 REFERENCES

[1] B. T. Åström. "*Manufacturing of Polymer Composites*". 1st edition, Routledge, 1997.

[2] L. C. Hollaway. "A review of the present and future utilisation of FRP composites in the civil infrastructure with reference to their important in-service properties". *Construction and Building Materials*, vol. 24, no. 12, pp. 2419–2445, 2010.

[3] T. F. A. Santos, G. C. Vasconcelos, W. A. de Souza, M. L. Costa, and E. C. Botelho. "Suitability of carbon fiber-reinforced polymers as power cable cores: Galvanic corrosion and thermal stability evaluation" *Materials & Design*, vol. 65, pp. 780–788, 2015.

[4] J. Galos, K. Pattarakunnan, A. S. Best, I. L. Kyratzis, C. H. Wang, and A. P. Mouritz. "Energy Storage Structural Composites with Integrated Lithium-Ion Batteries: A Review". *Advanced Materials Technologies*, vol. 6, no. 8, pp. 2001059, 2021.

[5] S. V. Hoa. "*Principles of the manufacturing of composite materials*". 1st edition, DEStech Publications, Inc, 2009.

[6] R. Li, W. Xu, D. Zhang, R. Li, W. Xu, and D. Zhang. "Impacts of Thermal and Mechanical Cycles on Electro-Thermal Anti-Icing System of CFRP Laminates Embedding Sprayable Metal Film". *Materials*, vol. 14, no. 7, pp. 1589, 2021.

[7] C. Karch and C. Metzner. "Lightning protection of carbon fibre reinforced plastics - An Overview". *33rd International Conference on Lightning Protection,* Portugal, pp. 1-8, 2016.

[8] A. S. Chen, D. P. Almond, and B. Harris. "Impact damage growth in composites under fatigue conditions monitored by acoustography". *International Journal of Fatigue*, vol. 24, no. 2–4, pp. 257–261, 2002.

[9] P. Tran, Q. T. Nguyen, and K. T. Lau. "Fire performance of polymer-based composites for maritime infrastructure". *Composites Part B: Engineering*, vol. 155, pp. 31–48, 2018.

[10] A. S. Verma, S. G. P. Castro, Z. Jiang, and J. J. E. Teuwen. "Numerical investigation of rain droplet impact on offshore wind turbine blades under different rainfall conditions: A parametric study". *Composite Structures*, vol. 241, pp. 112096, 2020.

[11] D. Tejero-Martin, M. Rezvani Rad, A. McDonald, and T. Hussain. "Beyond Traditional Coatings: A Review on Thermal-Sprayed Functional and Smart Coatings". *Journal of Thermal Spray Technology*, vol. 28, no. 4, pp. 598–644, 2019.

[12] R. Gonzalez, H. Ashrafizadeh, A. Lopera, P. Mertiny, and A. McDonald. "A Review of Thermal Spray Metallization of Polymer-Based Structures". *Journal of Thermal Spray Technology*, vol. 25, no. 5, pp. 897–919, 2016.

[13] A. Rezzoug, S. Abdi, A. Kaci, and M. Yandouzi. "Thermal spray metallisation of carbon fibre reinforced polymer composites: Effect of top surface modification on coating adhesion and mechanical properties". *Surface and Coatings Technology*, vol. 333, pp. 13–23, 2018.

[14] H. Che, X. Chu, P. Vo, and S. Yue. "Metallization of Various Polymers by Cold Spray". *Journal of Thermal Spray Technology*, vol. 27, no. 1–2, pp. 169–178, 2018.

[15] V. Bortolussi. "Cold spray of metal-polymer composite coatings onto carbon fiber-reinforced polymer (CFRP*)". International Thermal Spray Conference*, China, 2016.

[16] P. Fallah, S. Rajagopalan, A. McDonald, and S. Yue. "Development of hybrid metallic coatings on carbon fiber-reinforced polymers (CFRPs) by cold spray deposition of copper-assisted copper electroplating process". *Surface and Coatings Technology*, vol. 400, p. 126231, 2020.

[17] A. Lopera-Valle and A. McDonald. "Application of Flame-Sprayed Coatings as Heating Elements for Polymer-Based Composite Structures". *Journal of Thermal Spray Technology*, vol. 24, no. 7, pp. 1289–1301, 2015.

[18] A. Rahimi, M. Hojjati, A. Dolatabadi, and C. Moreau. “Thermal spray coating on polymeric composite for de-icing and anti-icing applications”. *Journal of Manufacturing Science and Engineering, Transactions of the ASME*, vol. 143, no. 10, 2021.

[19] J. Wigren. “Technical note: Grit blasting as surface preparation before plasma spraying”. *Surface and Coatings Technology*, vol. 34, no. 1, pp. 101–108, 1988.